Chronic exposure to asbestos enhances TGF-β1 production in the human adult T cell leukemia virus-immortalized T cell line MT-2

MEGUMI MAEDA[1,2], YING CHEN[2,4], HIROAKI HAYASHI[2,3], NAOKO KUMAGAI-TAKEI[2], HIDENORI MATSUZAKI[2], SUNI LEE[2], YASUMITSU NISHIMURA[2] and TAKEMI OTSUKI[2]

[1]Department of Biofunctional Chemistry, Graduate School of Environmental and Life Science, Okayama University, Okayama 7008530; Departments of [2]Hygiene and [3]Dermatology, Kawasaki Medical School, Kurashiki, Okayama 7010192, Japan; [4]Division of Pneumoconiosis, School of Public Health, China Medical University, Heping, Shenyang 110001, P.R. China

Received June 4, 2014; Accepted July 16, 2014

DOI: 10.3892/ijo.2014.2682

Abstract. Asbestos exposure causes various tumors such as lung cancer and malignant mesothelioma. To elucidate the immunological alteration in asbestos-related tumors, an asbestos-induced apoptosis-resistant subline (MT-2Rst) was established from a human adult T cell leukemia virus-immortalized T cell line (MT-2Org) by long-term exposure to asbestos chrysotile-B (CB). In this study, transforming growth factor-β1 (TGF-β1) knockdown using lentiviral vector-mediated RNA interference showed that MT-2Rst cells secreted increased levels of TGF-β1, and acquired resistance to TGF-β1-mediated growth inhibition. We showed that exposure of MT-2Org cells to CB activated the mitogen-activated protein kinases (MAPKs), ERK1/2, p38 and JNK1. Furthermore, TGF-β1-knockdown cells and treatment with MAPK inhibitors revealed that MT-2Rst cells secreted a high level of TGF-β1 mainly through phosphorylation of p38. However, an Annexin V assay indicated that TGF-β1 resistance in MT-2Rst cells was not directly involved in the acquisition of resistance to apoptosis that is triggered by CB exposure. The overall results demonstrate that long-term exposure of MT-2Org cells to CB induces a regulatory T cell-like phenotype, suggesting that chronic exposure to asbestos leads to a state of immune suppression.

Introduction

Exposure to asbestos (i.e., chrysotile, crocidolite or amosite) causes malignant mesothelioma (MM) and serious social problems (1-4). Therefore, early diagnosis of asbestos-related MM is required for early medical treatment because MM has an extremely poor prognosis. We reported previously that exposure to chrysotile asbestos causes immunological abnormalities in immunocompetent cells, such as T cells and NK cells, following research concerning identification of an early diagnosis indicator (5-10). In particular, the establishment of an *in vitro* experimental model of asbestos exposure using a human T-cell leukemia virus type-1 (HTLV-1)-immortalized human polyclonal T cell line, MT-2 (11), enabled analysis of immunological abnormalities induced by asbestos exposure and the identification of target molecules related to antitumor immunity (12-16). Actually, people exposed to asbestos usually have been receiving exposure from work or environmental circumstances extrinsically or from remaining fibers inhaled intrinsically. To establish an *in vitro* model of asbestos-exposure to immunocompetent cells, we have been using original MT-2 (MT-2Org) cells and examined short-term exposure as reported previously (13,14,17). The culturing of MT-2Org cells ($1x10^5$/2 ml of medium) with 0, 2.5, 5, 12.5 and 25 $\mu g/cm^2$ of chrysotile fibers was used to examine their growth features and the appearance of apoptosis measured by the TUNEL method. Growth inhibition and the appearance of apoptosis were dependent on dose and time (1-3 days) and resulted in the production of ROS, activation of pro-apoptotic MAPK signaling molecules such as p38 and JNK, and activation of the mitochondrial apoptotic pathway. However, relatively low doses (2.5 and 5 μg/ml) induced apoptosis in less than half of the cells. Thus, we continuously added these doses of chrysotile fibers to establish an *in vitro* cell line model of long-term exposure for more than eight months. Although short-term, high-dose exposure to asbestos causes apoptosis via a caspase-dependent pathway in original MT-2 cells, long-term (more than eight months) and low-dose (5 $\mu g/cm^2$) exposure to chrysotile-B (CB) results in resistance to apoptosis. Acquisition of resistance to CB occurs by increased Src family kinase-mediated interleukin-10 (IL-10) production, with subsequent activation of signal transducer and activator of transcription 3 (STAT3), and overexpression of anti-apoptotic protein Bcl-2 located down-stream of STAT3, resulting in the establishment of a CB-induced apoptosis-resistant subline (MT-2Rst) (14). Moreover, *bcl2* mRNA expression increases in peripheral $CD4^+$ T cells from MM patients, suggesting that MT-2Rst cells

Correspondence to: Dr Megumi Maeda, Department of Biofunctional Chemistry, Graduate School of Environmental and Life Science, Okayama University, 1-1-1 Tsushima-Naka, Okayama 7008530, Japan
E-mail: mmaeda@cc.okayama-u.ac.jp

Abbreviations: CB, chrysotile-B; Org, original; Rst, resistant; MM, malignant mesothelioma

Key words: asbestos chrysotile, SMAD, MAPK

are useful as a model for chronic CB exposure. Recently, we found reduced expression of cell surface chemokine receptor CXCR3 in MT-2Rst cells, and reported that the CXCR3 expression is decreased in peripheral $CD4^+$ T cells from patients with asbestos-related diseases such as pleural plaque or MM (18,19). Therefore, it is important to examine the cellular features of the MT-2Rst cell line to determine whether this subline has modified characteristics as immunocompetent cells which affect tumor immunity. On the other hand, MT-2Org cells are a regulatory T (Treg) cell-like cell line, as previously reported (20). Treg cells produce anti-inflammatory cytokine IL-10 and transforming growth factor-β1 (TGF-β1), which suppress antitumor immune function by inhibition of proliferation and differentiation of various immunocompetent cells (21,22).

In this study, we have shown that long-term exposure of MT-2Org cells to CB promotes a remarkable production of TGF-β1 through activation of chronic p38 mitogen-activated protein kinase (MAPK). In addition, MT-2Rst cells acquire resistance to TGF-β1-mediated growth inhibition. Our findings may indicate that increased production of IL-10 and TGF-β1 by chronic exposure to asbestos, and alteration of immunocompetent cells, may contribute to the development of asbestos-related MM by suppression of an antitumor immune system.

Materials and methods

Reagents. Recombinant human TGF-β1 was purchased from Peprotech, London, UK. PD98059 was obtained from Cell Signaling Technology, Inc., Danvers, MA, USA. SB203580 was acquired from Calbiochem, Madison, WI, USA. SP600125 was obtained from SABiosciences, Frederick, MD, USA.

Cell culture and asbestos. MT-2Org cells were kindly provided as a gift by the Cell Biology Institute, Research Center, Hayashibara Biochemical Laboratories, Inc. Okayama, Japan. MT-2Org cells were seeded in RPMI-1640 medium supplemented with 10% fetal bovine serum (FBS), streptomycin and penicillin. MT-2Rst cells were established from the MT-2Org cells by continuous exposure to CB (5 μg/cm^2) for more than eight months as previously described (12,14). 293FT cells were cultured in Dulbecco's modified Eagle's medium (Invitrogen, Carlsbad, CA, USA) supplemented with 10% FBS. The UICC (the International Union Against Cancer) standard of CB was kindly provided by the Department of Occupational Health, National Institute for Occupational Health, South Africa (23). Chrysotile asbestos is composed of $Mg_3Si_2O_5$ $(OH)_4$. Chrysotile-A from Zimbabwe contains 2% fibrous anthophyllite, although CB from Canada does not contain any fibrous impurities.

Real-time RT-PCR analysis. Total RNA was extracted from cells using the RNeasy mini kit (Qiagen, Hilden, Germany), and cDNAs were synthesized using the PrimeScript II® 1st strand cDNA Synthesis kit (Takara, Shiga, Japan), according to the manufacturer's instructions. Real-time RT-PCR was performed using Brilliant II Fast SYBR® Green QPCR Master Mix (Stratagene, La Jolla, CA, USA) with the Mx3000P QPCR System (Agilent Technologies Inc.), according to the manufacturer's instructions. Real-time RT-PCR of the TGF-β1 primers were 5'-TTCAACACATCAGAGCTCCG-3' (forward) and 5'-ATAACCACTCTGGCGAGTCG-3' (reverse), for TGF-βRI: 5'-TAATTCCTCGAGATAGGCCG-3' (forward) and 5'-TCGATGGTGAATGACAGTGC-3' (reverse), for TGF-βRII: 5'-CAGCAGAAGCTGAGTTCAACC-3' (forward) and 5'-GTGTTCTGCTTCAGCTTGGC-3' (reverse), for SMAD2: 5'-GGAATTTGCTGCTCTTCTGG-3' (forward) and 5'-TCTGCCTTCGGTATTCTGCT-3' (reverse), for SMAD3: 5'-CCCCAGAGCAATATTCCAGA-3' (forward) and 5'-GGCTCGCAGTAGGTAACTGG-3' (reverse), for GAPDH: 5'-GAGTCAACGGATTTGGTCGT-3' (forward) and 5'-TTGATTTTGGAGGGATCTCG-3' (reverse). The relative gene expression was calculated by the ΔΔCt method using an endogenous control (GAPDH) as 1.0. The formula is expressed as follows: $2^{-\Delta\Delta Ct} = 2^{-(\Delta Ct \text{ for target gene} - \Delta Ct \text{ for GAPDH})}$.

ELISA. Cultured cells were purified using the Ficoll-Paque method to remove CB. Cells ($2x10^5$/ml) were cultured in 24-well plates in RPMI-1640 medium supplemented with 10% 1X Serum Replacement 1 (Sigma-Aldrich) for 3 days. Levels of TGF-β were quantified by immunoassay using Quantikine ELISA kits (R&D Systems, Minneapolis, MN, USA) according to the manufacturer's instructions.

Flow cytometry. Cell surface proteins were stained with anti-human latency associated peptide (LAP) (TGF-β1)-PE antibody (27232) or anti-human TGF-βRII-PE antibody (FAB241P) (R&D Systems). Analysis was performed by a flow cytometer (FACSCalibur™; BD Biosciences, Franklin Lakes, NJ, USA). For intracellular staining of TGF-β1, cell surface TGF-β1 was blocked with 2.5 μg/ml of anti-human TGF-β1 antibody (9016) (R&D Systems) for 30 min at room temperature. Cells were fixed and permeabilized using a fixation/permeabilization solution (BD Biosciences) for 20 min at 4˚C. After washing twice in BD Perm/Wash buffer (BD Biosciences), cells were stained with anti-human TGF-β1-PE (9016) (R&D Systems) for 30 min at 4˚C. After washing with BD Perm/Wash buffer, cells were resuspended in PBS and analyzed on a flow cytometer.

Cell growth. Cultured MT-2Org cells, MT-2Rst cells, MT-2Org control cells, MT-2Rst control cells, and TGF-β1-knockdown in MT-2Rst cells were purified using the Ficoll density gradient method to remove CB completely, and cells were then cultured for 2-4 days in the absence of CB. Cells ($2x10^4$/100 μl) were cultured in 96-well U-bottom plates in RPMI-1640 medium supplemented with 10% 1X Serum Replacement 1 (Sigma-Aldrich) in the presence or absence of TGF-β1. The proliferation was evaluated on day 3 based on [^{3}H]-thymidine incorporation. After 2 days of culture, 3.7 kBq (0.1 μCi) [^{3}H]-thymidine (10 μl) (GE Healthcare UK Ltd., Buckinghamshire, UK) was added to each well. After 16 h of culture, [^{3}H]-thymidine incorporation was measured using a liquid scintillation counter (LSC-5100, Aloka, Japan).

Western blot analysis. Cells were lysed in 50 mM Tris-HCl (pH 7.2) buffer containing 150 mM NaCl, 1% Nonidet P-40, 1% deoxycholic acid, 0.05% sodium dodecyl sulfate (SDS), 1X protease inhibitor cocktail (Sigma-Aldrich, St. Louis, MO, USA), and 1X Halt Phosphatase Inhibitor Cocktail (Thermo Fisher Scientific Inc., Rockford, IL, USA). Proteins were

quantified using the BCA assay kit (Thermo Fisher Scientific Inc.), and 10 μg of protein was resolved on 10% SDS-PAGE under reducing conditions with 5% 2-mercaptoethanol and transferred to a PVDF membrane. Proteins were probed with the following antibodies: p-SMAD2, p-SMAD3, SMAD2/3 (Cell Signaling Technology, Inc.), p-ERK, p-JNK, ERK1, JNK1/3, p38α, (Santa Cruz Biotechnology, Santa Cruz, CA, USA), p-p38 (BD Biosciences, San Jose, CA, USA), and GAPDH (Millipore Corp. Headquarters, Billerica, MA, USA), and incubated with HRP-conjugated anti-mouse IgG or anti-rabbit IgG (Santa Cruz Biotechnology). Proteins were detected with ECL Plus Western Blotting Detection Reagents (GE Healthcare UK Ltd.). The intensity of western blotting was quantified with Dolphon-View2 Band Tool (Kurabo Industries Ltd, Osaka, Japan).

RNA interference. Three kinds of double-stranded oligonucleotides 5'-GATCCCCGGAGGTCACCCGCGTGCTATTCAAGAGATAGCACGCGGGTGACCTCCTTTTTGGAAA-3' (no. 1), 5'-GATCCCCGTTCAAGCAGAGTACACACTTCAAGAGAGTGTGTACTCTGCTTGAACTTTTTGGAAA-3' (no. 2) and 5'-GATCCCCGTGGACATCAACGGGTTCATTCAAGAGATGAACCCGTTGATGTCCACTTTTTGGAAA (no. 3) were subcloned into pSUPER digested by *Bgl*II-*Hin*dIII (24). Resulting constructs were digested with *Bam*HI/*Sal*I, and short hairpin RNA (shRNA) containing human H1 RNA polymerase III promoter subcloned into the *Bam*HI-*Sal*I site of pRDI292 as described previously (25).

Lentiviral vector production and viral infection. The vesicular stomatitis virus G protein (VSV-G)-pseudotyped HIV-1-based vector system was generated as described previously (26). The Replication-defective lentiviral vector particles were produced by transient cotransfection of the second-generation packaging construct pCMV-ΔR8.91 (27), the VSV-G envelope plasmid pMDG2 and the lentiviral vector into 293FT cells with FuGENE6 (Roche Diagnostics, Mannheim, Germany). The supernatant containing the virus was collected 48 and 72 h after transfection. The lentivirus-containing supernatants were subjected to MT-2Org and MT-2Rst cells ($0.5x10^5$ in 2 ml of medium) in a 6-well plate. After 3 days, cells were treated with 1 μg/ml of puromycin to select stable clones expressing the shRNA.

Analysis of apoptosis by Annexin V staining. Cells ($1x10^5$/ml) were cultured in the absence or presence of 5, 12.5 or 25 $\mu g/cm^2$ CB in 24-well plates for 24 h. Apoptotic cells were detected by staining with Annexin V-FITC and propidium iodide (PI) (Roche Applied Science, Indianapolis, IN, USA) according to the manufacturer's protocol, and stained cells were analyzed using a flow cytometer.

Statistical analysis. A t-test and a Fisher's parametric least significant difference (PLSD) were performed to determine statistical differences between the experimental groups.

Results

Enhancement of TGF-β1 production in MT-2Rst cells by continuous exposure to CB. Long-term exposure to CB results in CB-dependent resistance to apoptosis and upregulates IL-10 production in MT-2Org cells, as previously described (14). Given that MT-2Org cells are known to have a Treg cell-like suppressive function (20), in this study we investigated the production of an anti-inflammatory cytokine, TGF-β1, in MT-2Rst cells by long-term exposure to CB. The production of TGF-β1 in culture supernatants was augmented large in MT-2Rst compared to MT-2Org cells (Fig. 1B). Besides FACS analysis showed that intracellular TGF-β1 was strongly expressed in both MT-2Org and MT-2Rst cells as shown in the middle and bottom panels of Fig. 1A, but there were no significant differences such as those revealed by real-time RT-PCR (top panel of Fig. 1A). Additionally, the cell surface TGF-β1 expression was increased in MT-2Rst cells, although there were no significant differences between MT-2Org and MT-2Rst cells (Fig. 1C). MT-2 cells are HTLV-1-immortalized human polyclonal T cell line and express Tax protein which represses TGF-β1 signaling in human T cells (28). Although we compared the gene expression level of Tax1 between MT-2Org and MT-2Rst cells, there were no differences in the gene expression level (data not shown). These results suggested that the upregulation of TGF-β1 production in MT-2Rst cells induced by long-term exposure to CB leads to an enhancement of Treg-like phenotypes in a Tax-independent manner.

MT-2Rst cells acquire resistance to the growth inhibitory effect of TGF-β1. Although TGF-β1 inhibits the proliferation of T cells and NK cells, TGF-β1 does not inhibit the growth of TGF-β1-producing Treg cells (29). Therefore, we examined whether TGF-β1 inhibits the proliferation of MT-2Rst cells. As shown in Fig. 2A, the proliferation of MT-2Org cells was significantly inhibited by TGF-β1, whereas MT-2Rst cells were not inhibited. In order to confirm whether the resistance to TGF-β1-mediated growth inhibition depends on TGF-β1 production, TGF-β1 knockdown in MT-2Rst cells was generated using lentiviral vector-mediated RNA interference. The knockdown efficiency of three TGF-β1 shRNA constructs was examined by real-time RT-PCR and ELISA (Fig. 3A), and the results confirmed that the expression of *TGF-β1* mRNA and production of TGF-β1 significantly decreased in construct nos. 1 and 2. Therefore, these cell clones (construct nos. 1 and 2) were employed in subsequent experiments. Interestingly, TGF-β1-knockdown cells significantly inhibited their proliferation by TGF-β1 treatment in a manner similar to the MT-2Org control transduced with a control lentiviral vector, although these growth suppressions due to TGF-β1 were not observed in MT-2Rst control cells transduced with a control lentiviral vector (Fig. 3B). These results suggested that MT-2Rst cells acquired the resistance to TGF-β1-mediated growth inhibition through upregulation of TGF-β1 production.

Next, we investigated the expression of TGF-β receptor (R) I and TGF-βRII in MT-2Org and MT-2Rst cells to elucidate a mechanism in which TGF-β1 did not inhibit the growth of TGF-β1-producing MT-2Rst cells. Real-time RT-PCR revealed that both cells expressed *TGF-βR1* and *TGF-βR2* mRNA, and that the latter expression was significantly decreased in MT-2Rst cells (Fig. 2B). However, FACS analysis showed that the expression of cell surface TGF-βRII was low in both cells and there were no significant differences

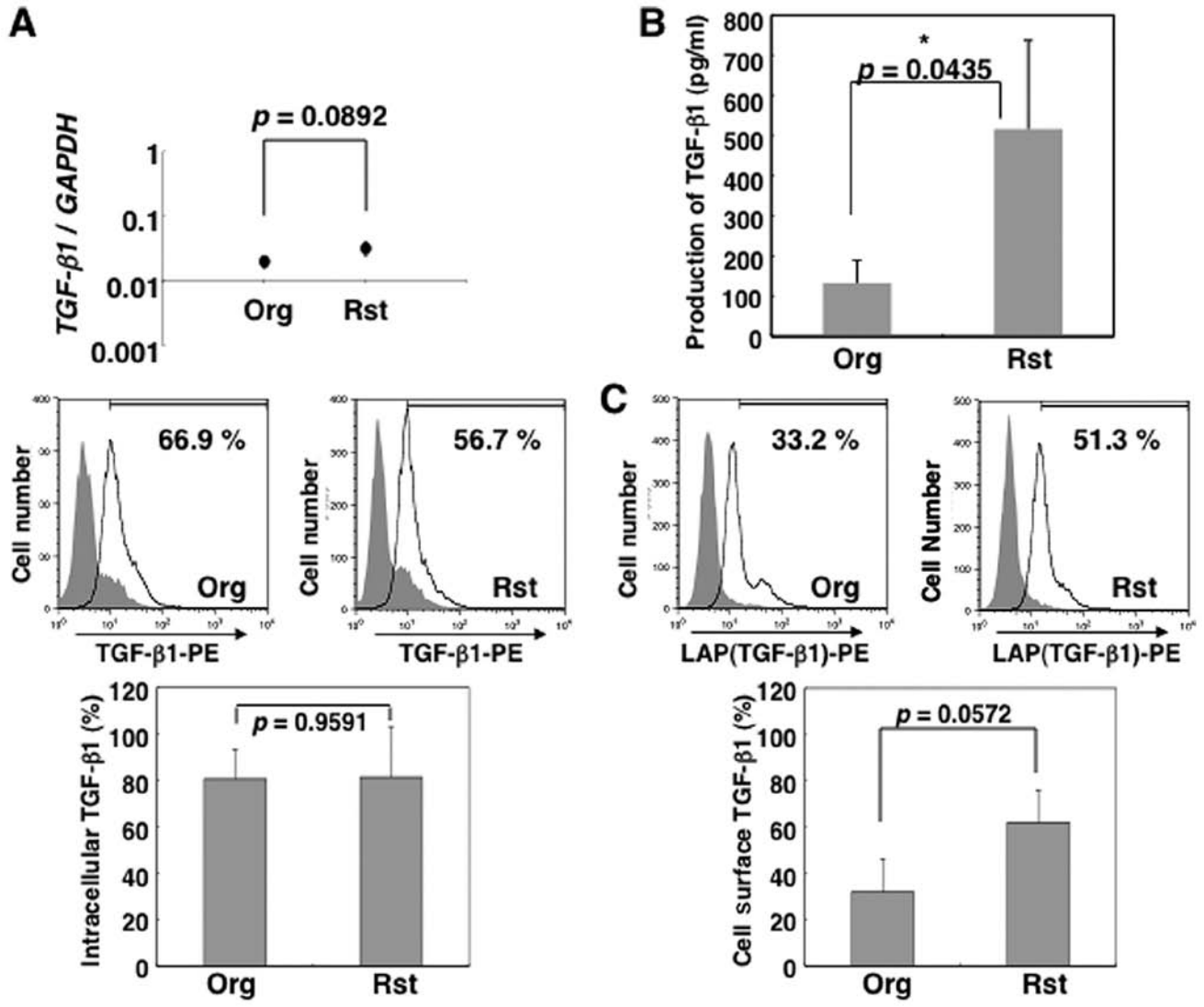

Figure 1. Long-term exposure of MT-2Org cells to CB enhances Treg-like phenotypes. MT-2Rst cells (Rst) were established from MT-2Org cells (Org) by long-term exposure to CB. (A) Relative mRNA expression of *TGF-β1* was estimated by real-time RT-PCR (top). Representative histograms show intracellular TGF-β1 expression (middle). The gray plot shows data from an unstained control. The graph shows comparison of the proportion of TGF-β1$^+$ cells (bottom). Results represent the mean ± SD from three independent experiments. The p-value was obtained using Fisher's PLSD test. (B) Activated TGF-β1 levels in culture supernatants were assessed by ELISA. Error bars represent SD from three independent experiments. The p-value was obtained using Fisher's PLSD test. *p<0.05. (C) Representative histograms show cell surface LAP (TGF-β1) expression. The gray plot shows data from an unstained control. The graph shows comparison of the proportion of LAP (TGF-β1)$^+$ cells. Results represent the mean ± SD from three independent experiments. The p-value was obtained using Fisher's PLSD test.

(Fig. 2B). Additionally, expression of *TGF-βR1* and *TGF-βR2* mRNA decreased in MT-2Rst control cells was enhanced in TGF-β1-knockdown cells, and was particularly remarkable in construct no. 1 when compared with the MT-2Rst control cells (Fig. 3C). These results suggested that the acquisition of the resistance to TGF-β1-mediated growth inhibition might be partly associated with the expression level of TGF-βRI/II.

TGF-β1 production in MT-2Rst cells via p38 MAP kinase activation. To elucidate the molecular mechanism involved in overexpression and over-production of TGF-β1 in MT-2Rst cells, we investigated the importance of these aspects and the activation of MAPKs, such as ERK1/2, p38 and JNK1. Given that we previously reported that exposure to chrysotile-A induces apoptosis via phosphorylation of p38 and JNK (13), we examined the activation of MAPKs in MT-2Org cells subjected to short-term exposure to CB. As shown in Fig. 4, ERK1/2, p38 and JNK1 were phosphorylated when MT-2Org cells were exposed to 5 or 12.5 μg/cm^2 of CB, although there were no significant differences between the treated and control groups. Furthermore, as shown in Fig. 5A and B, phosphorylated p38 in MT-2Rst control was decreased by knockdown of TGF-β1. To confirm the association between TGF-β1 production and p38 MAP kinase activation, MT-2Rst cells were treated with ERK inhibitor PD98059, p38 MAP kinase inhibitor SB203580, or JNK inhibitor SP600125. As shown in Fig. 5C, TGF-β1 production was largely reduced by inhibition of p38 phosphorylation, while decreased TGF-β1 production was also induced by inhibition of ERK and JNK phosphorylation involved in proliferation of cells (30). These results

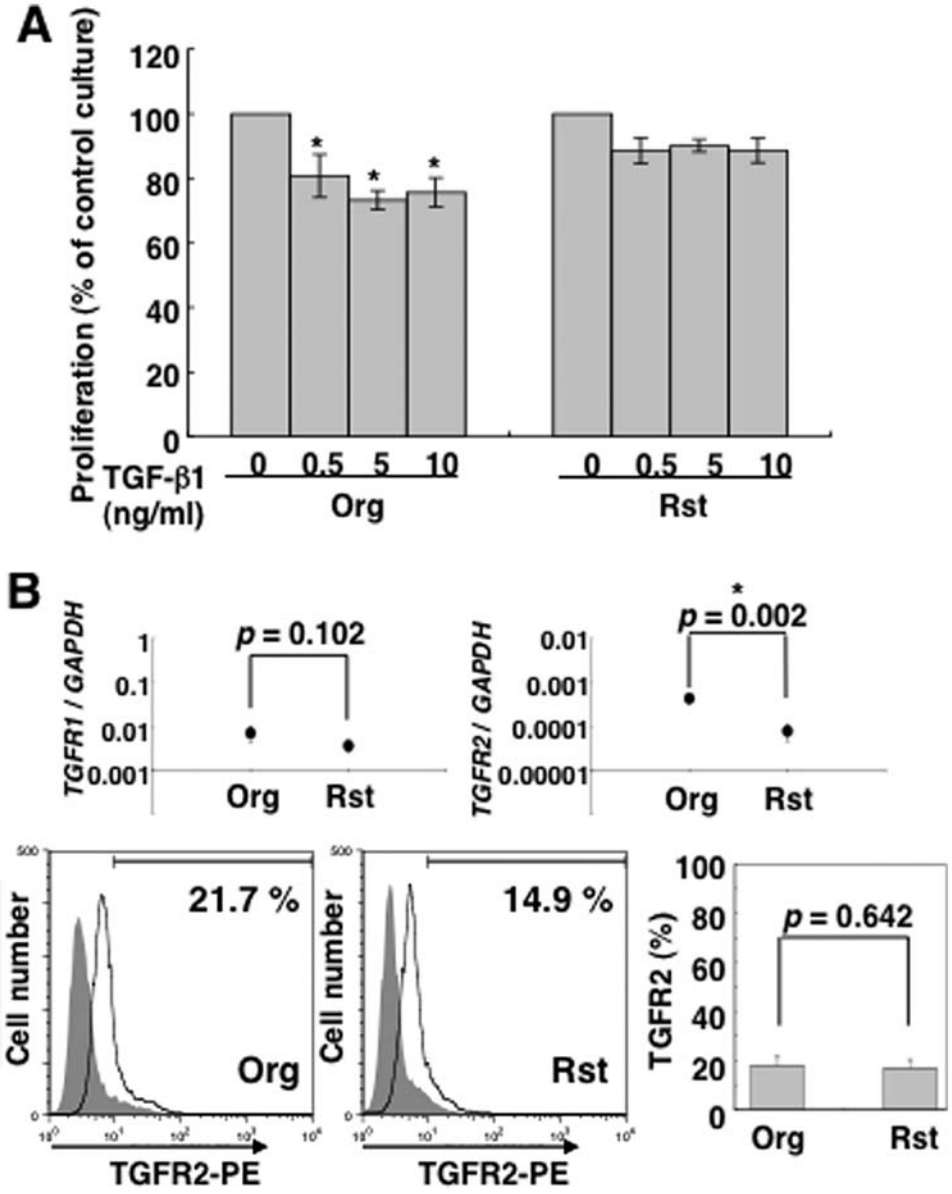

Figure 2. MT-2Rst cells exhibit resistance to TGF-β1-mediated growth inhibition via downregulation of TGF-β receptors. (A) Effect of TGF-β1 treatment on proliferation of MT-2Org and MT-2Rst cells. The proliferation of untreated cells was set at 100%. Results represent the mean ± SD from three independent experiments. The p-value was obtained using Fisher's PLSD test. *p<0.001. (B) Relative mRNA expression of *TGF-βR1* and *TGF-βR2* was estimated by real-time RT-PCR. Representative histograms show TGF-βRII expression. The gray plot shows data from an unstained control. Graph shows comparison of the proportion of TGF-βRII$^+$ cells. Results represent the mean ± SD from three independent experiments. The p-value was obtained using Fisher's PLSD test. *p<0.01.

suggested that long-term exposure to CB upregulates TGF-β1 production via constitutive activation of the phosphorylation of p38.

Apoptosis induced by CB occurs independently of increased TGF-β1 production. To determine whether MT-2Rst cells acquire resistance to asbestos-induced apoptosis depending on the modification of TGF-β1 production, we examined the occurrence of apoptosis caused by co-culturing with CB in TGF-β1-knockdown cells using the Annexin V method. As shown in Fig. 6A, the short-term and high-dose exposure to CB did not induce apoptosis in TGF-β1-knockdown cells as in the MT-2Rst control cells, not knocked down, when compared with the appearance of apoptosis in MT-2Org cells. The short-term and high-dose exposure to CB in MT-2Org cells slightly increased in TGF-β1 production via apoptosis, although there were no significant differences between the treated and control groups (Fig. 6B). These results indicated that acquisition of resistance to CB-induced apoptosis in MT-2Rst cells occurs independently of enhanced TGF-β1 production by long-term exposure to CB.

Regulation of Smad-dependent TGF-β1 signaling in MT-2Rst cells. TGF-β1-Smad pathway is involved in the inhibition of T cell proliferation (31-34). We examined that the expression and phophorylation of SMAD2/3 in TGF-β1 producing MT-2Rst cells. SMAD2 was highly expressed at mRNA and protein levels in MT-2Org and MT-2Rst cells, and the level

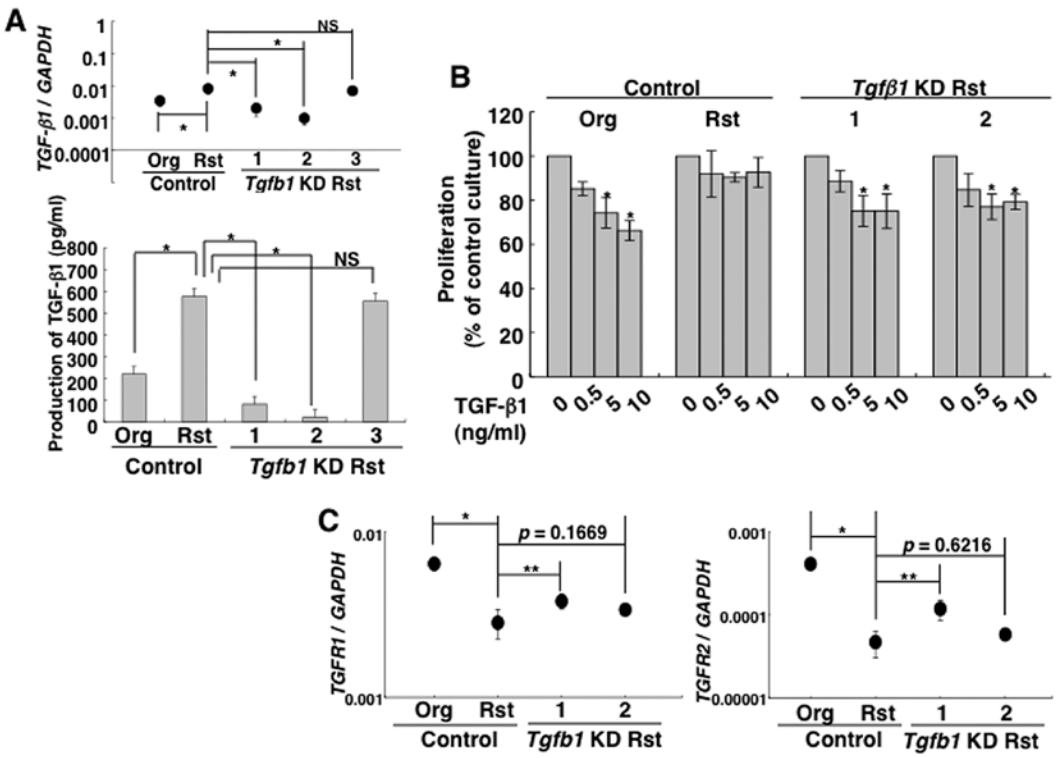

Figure 3. Enhanced TGF-β1 production associated with acquisition of resistance to TGF-β1-mediated growth inhibition. TGF-β1 knockdown in MT-2Rst cells using lentiviral vector-mediated RNA interference was performed as described in Materials and methods. MT-2Org and MT-2Rst control cells were generated with a control lentiviral vector. (A) Relative mRNA expression of *TGF-β1* was estimated by real-time RT-PCR (top). Activated TGF-β1 levels in culture supernatants were assessed by ELISA (bottom). Error bars represent SD from three independent experiments. The p-value was obtained using Fisher's PLSD test. *p<0.01. (B) Effect of TGF-β1 treatment on proliferation of TGF-β1 knockdown MT-2Rst cells. The proliferation of untreated cells was set at 100%. Results represent the mean ± SD from three independent experiments. The p-value was obtained using Fisher's PLSD test. *p<0.001. (C) Relative mRNA expression of *TGF-βR1* and *TGF-βR2* was estimated by real-time RT-PCR. Results represent the mean ± SD from three independent experiments. The p-value was obtained using Fisher's PLSD test. *p<0.01, **p<0.05.

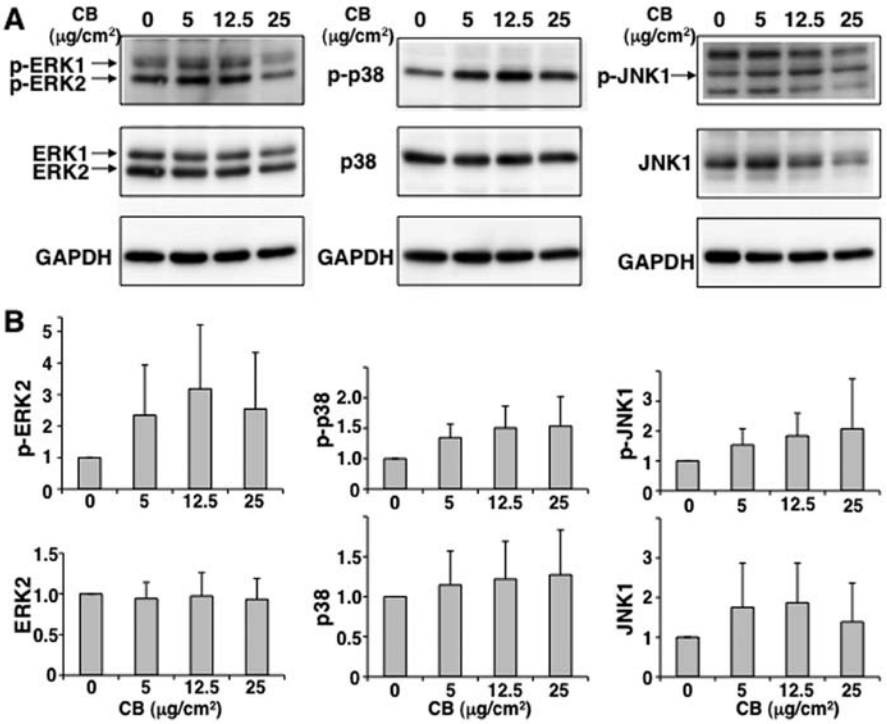

Figure 4. MAPKs, ERK, p38 and JNK on MT-2Org cells are activated by exposure to CB. (A) MT-2Org cells ($1x10^5$/ml) were cultured in the absence or presence of 5, 12.5 or 25 $\mu g/cm^2$ CB in RPMI-1640 medium supplemented with 10% FBS for 24 h. Expression and phosphorylation of ERK1/2, p38 and JNK1 were detected by western blotting. GAPDH was detected as a loading control. Data are representative of three experiments. (B) The levels of protein and phosphorylation on western blotting were quantified by densitometry. Quantitative results were normalized by GAPDH, and the relative expression of MT-2Org cells was defined as one. Results represent the mean ± SD from three independent experiments. The p-value was obtained using Fisher's PLSD test.

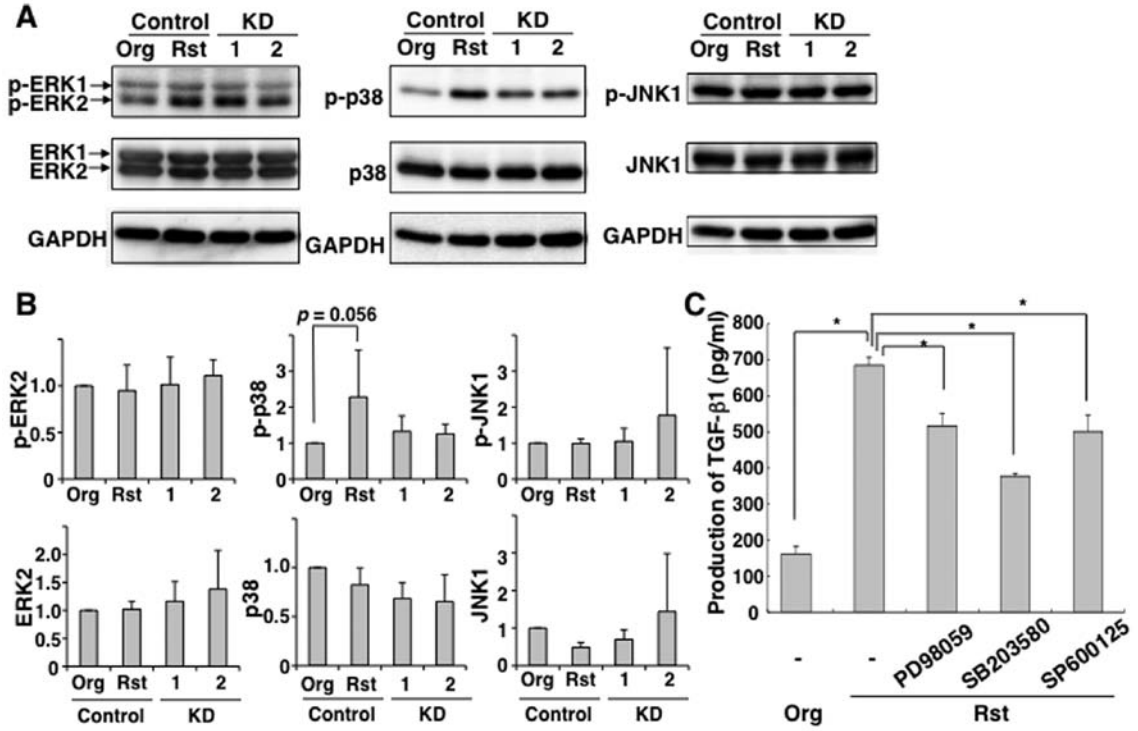

Figure 5. Production of TGF-β1 in MT-2Rst cells is dependent on activation of p38. (A) Expression and phosphorylation of ERK1/2, p38 and JNK1 were detected by western blotting. GAPDH was detected as a loading control. Data are representative of three experiments. (B) The levels of protein and phosphorylation on western blotting were quantified by densitometry. Quantitative results were normalized by GAPDH, and the relative expression of MT-2Org cells was defined as 1. Results represent the mean ± SD from three independent experiments. The p-value was obtained using Fisher's PLSD test. (C) MT-2Rst cells were cultured with 30 μM PD98059, 30 μM SB203580, 30 μM SP600125 or a vehicle control (dimethyl sulfoxide, DMSO) for 72 h. Activated TGF-β1 levels in culture supernatants were assessed by ELISA. Error bars represent SD from three independent experiments. The p-value was obtained using Fisher's PLSD test. *p<0.001.

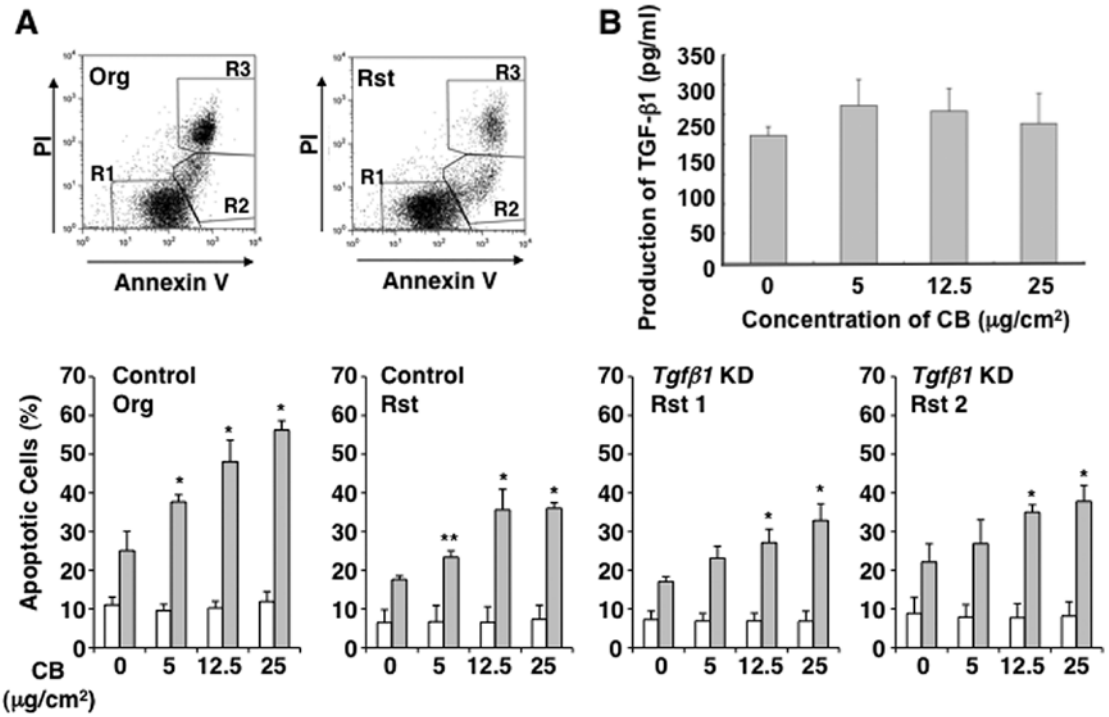

Figure 6. Upregulation of TGF-β1 production in MT-2Rst cells is not related to acquisition of resistance against apoptosis induced by CB exposure. (A) TGF-β1 knockdown MT-2Rst cells were cultured in the absence or presence of 5, 12.5 or 25 μg/cm^2 CB. After 24 h, cells were subjected to the Annexin V assay (FACS profiles shown in top panel). Region 1 (R1) represents viable cells (Annexin V$^-$/PI$^-$), region 2 (R2) early apoptotic cells (Annexin V$^+$/PI$^-$), and region 3 (R3) late apoptotic cells (Annexin V$^+$/PI$^+$). The graph shows the percentage of apoptotic cells (bottom). Open bars and gray bars show [R2/(R1 + R2 +R3)] and [(R2 + R3)/(R1 + R2 + R3)], respectively. At least three independent experiments are averaged, and data are expressed as the mean ± SD. The p-value was obtained using Fisher's PLSD test. **p<0.05, *p<0.01. (B) MT-2Org cells were cultured in the absence or presence of 5, 12.5 or 25 μg/ml CB for 72 h. Activated TGF-β1 levels in culture supernatants were assessed by ELISA. Error bars represent SD from three independent experiments. The p-value was obtained using Fisher's PLSD test. *p<0.05.

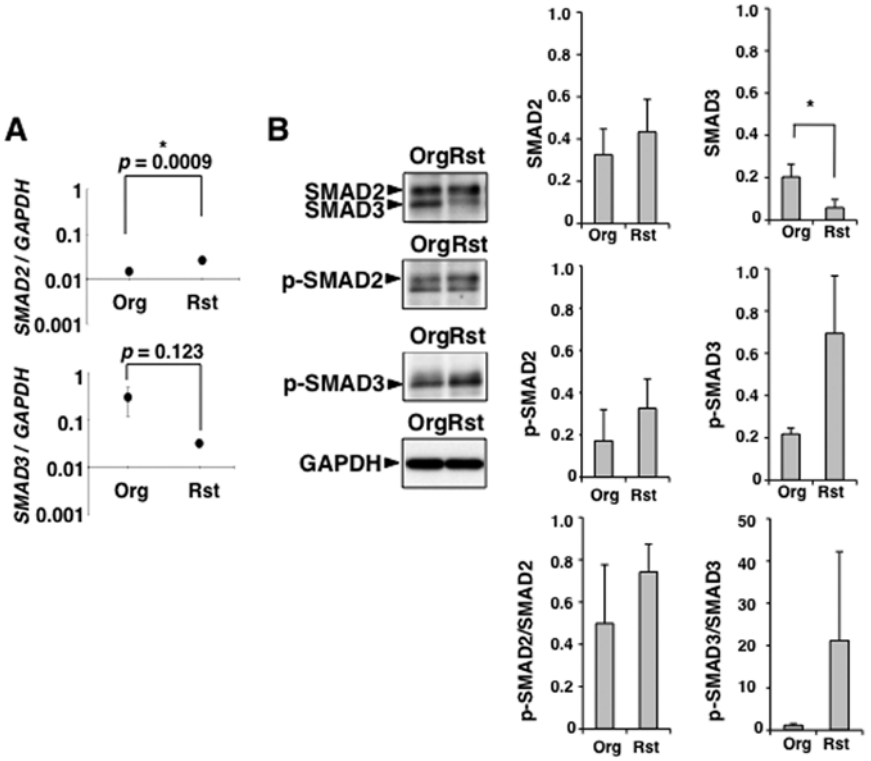

Figure 7. Long-term exposure to CB in MT-2Org cells has an effect on the expression and phosphorylation of SMAD2/3 in MT-2Rst cells. (A) Relative mRNA expression of *SMAD2* and *SMAD3* was estimated by real-time RT-PCR. Results represent the mean ± SD from three independent experiments. The p-value was obtained using Fisher's PLSD test. *p<0.01. (B) Expression and phosphorylation of SMAD2/3 protein were detected by western blotting. GAPDH was detected as a loading control. The levels of protein and phosphorylation on western blotting were quantified by densitometry. Quantitative results were normalized by GAPDH. Results represent the mean ± SD from three independent experiments. The p-value was obtained using t-test. *p<0.05.

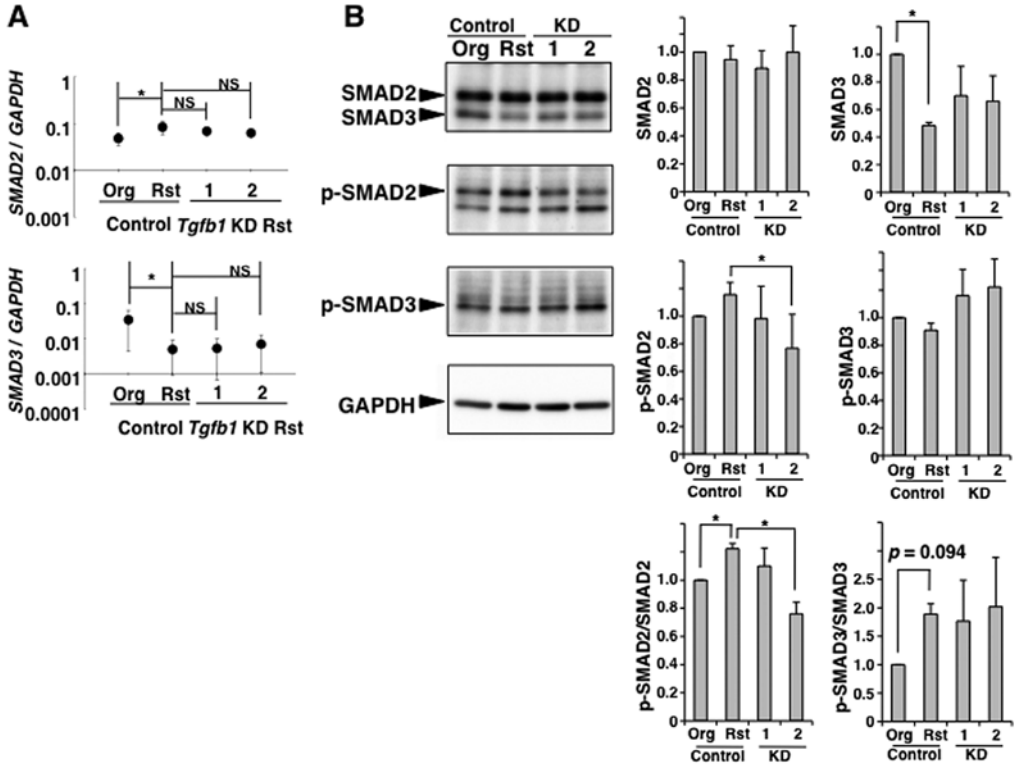

Figure 8. TGF-β1 production in MT-2Rst cells has no effect on *SMAD2/3* mRNA expression. (A) Relative mRNA expression of *SMAD2* and *SMAD3* was estimated by real-time RT-PCR (left). Results represent the mean ± SD from three independent experiments. The p-value was obtained using Fisher's PLSD test. *p<0.05. Expression and phosphorylation of SMAD2/3 protein were detected by western blotting. GAPDH was detected as a loading control (right). Data are representative of three experiments. (B) The levels of protein and phosphorylation on western blotting were quantified by densitometry. Quantitative results were normalized by GAPDH, and the relative expression of MT-2Org cells was defined as one. Results represent the mean ± SD from three independent experiments. The p-value was obtained using Fisher's PLSD test. *p<0.05.

of *SMAD2* mRNA was significantly higher in MT-2Rst than MT-2Org cells (Fig. 7A). Similarly, in Fig. 8, there were no significant differences in the protein level of SMAD2 arising from the level of *SMAD2* mRNA between MT-2Org control and MT-2Rst control cells, suggesting that SMAD2 is degraded by proteasome to maintain a certain amount of SMAD2 protein (35). On the other hand, mRNA and protein expression levels of SMAD3 were lower in MT-2Rst than MT-2Org cells, and the protein level of SMAD3 was significantly decreased in MT-2Rst compared with MT-2Org cells (Fig. 7). Similarly, the mRNA and protein level of SMAD3 were significantly decreased in MT-2Rst cells (Fig. 8). SMAD2/3 was highly phosphorylated in MT-2Rst cells compared with MT-2Org cells (Fig. 7B), although the level of phosphorylated SMAD3 was not enhanced in MT-2Rst cells (Fig. 8). The level of phosphorylated SMAD2 (p-SMAD2) and SMAD3 (p-SMAD3) were normalized to the protein expression level of SMAD2 and SMAD3, respectively. The levels of p-SMAD2/SMAD2 and p-SMAD3/SMAD3 were increased in MT-2Rst cells compared with MT-2Org cells (Figs. 7B and 8), suggesting that Smad-dependent TGF-β1 signaling through the activation of TGF-βRI/II stimulated by autocrine TGF-β1 from MT-2Rst cells was performed normally in MT-2Rst cells.

However, the results from TGF-β1-knockdown in MT-2Rst cells showed that there were no significant differences in mRNA expression of *SMAD2* and *SMAD3* among MT-2Rst control, TGF-β1-knockdown nos. 1 and 2 (Fig. 8). Whereas the level of p-SMAD2/SMAD2 was decreased in TGF-β1-knockdown cells, and was particularly remarkable in construct no. 2 when compared with the MT-2Rst control cells (Fig. 8B). The SMAD3 protein expression decreased in the MT-2Rst control was recovered slightly by TGF-β1-knockdown, although there were no differences in p-SMAD3/SMAD3 among MT-2Rst control, TGF-β1-knockdown nos. 1 and 2. Thus, phosphorylation of SMAD2 and SMAD3 may be coordinated with the expression of SMAD2 and SMAD3. These results were insufficient to understand that long-term exposure of MT-2Org cells to CB induces TGF-β1 production, and results in acquisition of the resistance to TGF-β1-mediated growth inhibition.

Discussion

In this study, it was revealed that MT-2Rst cells, which were established from MT-2Org cells by continuous exposure to CB, produced high levels of TGF-β1 through phosphorylation of p38 MAPK, and acquire resistance to inhibition of cell growth by TGF-β1. Moreover, it was suggested that continuous exposure of the $CD4^+CD25^+$ HTLV-1 immortalized T cell line (MT-2Org cells) to CB induces modification of cellular phenotypes and makes these cells resemble Treg cells.

TGF-β1 inhibits proliferation and differentiation of various immunocompetent cells, resulting in suppression of antitumor immune function (22,29). On the other hand, TGF-β1 has contributed to the development of induced Treg cells (36). Therefore, induced Treg cells that have the ability to produce TGF-β1 do not exhibit inhibited cell growth by TGF-β1. Given that TGF-β1 is produced not only from Treg cells but also tumor cells, including MM cells (37), the tumor microenvironment is rich in TGF-β1 (38) and results in the proliferation of MM cells by TGF-β1 (39). Consequently, TGF-β1 derived from Treg cells and tumor cells, which inhibits the antitumor function of immune cells, induces an immunosuppressive microenvironment surrounding the tumor and promotes tumor growth. Plasma from patients with MM has high TGF-β1 levels, as previously reported (40). Our findings suggest that long-term exposure to asbestos induces T cells that exhibit resistance to the inhibitory effect against T cell proliferation by TGF-β1 derived from tumor cells, resulting in TGF-β1 development of Treg cells, suppression of antitumor immune function, and enhancement of tumor growth. We need additional investigations of Treg cells in MM patients to elucidate the immunosuppressive state induced by TGF-β1.

TGF-β1 signaling depends on a heteromeric complex of two types of transmembrane serine/threonine kinase receptors (41). TGF-β1 binds to the receptor complex, which activates TGF-βRII kinase to phosphorylate and activate TGF-βRI kinase. The activated TGF-βRI phosphorylates SMAD2 and SMAD3. Once SMAD2 or SMAD3 has been phosphorylated, it interacts with SMAD4, and the complex translocates to the nucleus, where it associates with other transcription factors to activate transcription of target genes (42). It is known that mutations of SMAD2/3 are involved with the progression of cancer (43,44). In this study, Smad-dependent TGF-β1 signaling operated correctly in MT-2Rst cells. Therefore, it seemed that the acquisition of resistance to TGF-β1 in MT-2Rst cells caused by the long-term exposure to CB due to reduced mRNA expression of TGF-β1 receptors in a Smad-independent manner. Furthermore, it was observed that the acquisition of resistance to the cell-proliferation inhibition effects of TGF-β1 through increased TGF-β1 production in MT-2Rst cells might not directly participate in the acquisition of resistance to apoptosis induced by CB exposure.

It is known that apoptotic cells secrete TGF-β1 (45). Given that induced Treg cells were developed by TGF-β1, we examined the relation between TGF-β1 production and apoptosis in MT-2 cells. However, the results suggested that TGF-β1 production was not related to apoptosis by exposure to asbestos. On the other hand, it has been reported that the conversion of $CD4^+CD25^-$ T cells into induced Treg cells is mediated by activation of p38 MAPK (46). Interestingly, phosphorylation of p38 in MT-2Rst cells increased markedly, which was decreased by TGF-β1 knockdown. Furthermore, TGF-β1 production in MT-2Rst cells decreased by treatment with the p38 inhibitor, suggesting that MT-2Org cells secrete TGF-β1 through constitutive phosphorylation of p38 due to chronic exposure to CB. Finally, MT-2Rst cells became much more similar to the Treg-like cell phenotype.

It is thought that MT-2Org cells are Treg-like cells, since MT-2 cells possess a high level of forkhead box P3 (Foxp3) and exhibit suppressive activity in relation to T cell proliferation (20). Our findings have shown that long-term exposure of MT-2Org cells to CB enhanced increased production of anti-inflammatory cytokine IL-10 and TGF-β1. Therefore, it would be necessary to analyze expression of Treg cell-related molecules [Foxp3, cytotoxic T-lymphocyte antigen 4 (CTLA-4), glucocorticoid-induced TNF-receptor (GITR)], and the suppressive function of T cell proliferation in MT-2Rst cells (21). In fact, Italian group has recently reported that CTLA-4 had been used as a target for treatment of advanced malignant

mesothelioma (47). Furthermore, given that we have found that the TGF-β1 production in MT-2Rst cells was induced by chronic exposure to chrysotile-A and crocidolite, it would be interesting to determine whether immunocompetent cells are affected depending on the asbestos character (data not shown).

Taken together, these results may indicate the possibility of using TGF-β1, TGF-βRI/II and SMAD2/3 as target molecules in $CD4^+$ T cells for the diagnosis and treatment of asbestos-related MM.

Acknowledgements

We thank Dr Yasuo Ariumi for the VSV-G-pseudotyped HIV-1-based vector system (pCMVΔR8.91 and pMDG2), pSUPER, pRDI292, and 293FT cells. We also thank Misao Kuroki for technical assistance. The authors thank the former members of our department, Dr Yoshie Miura, Shuko Murakami, Fuminori Hyodoh, Akiko Takata-Tomokuni and Ayako Ueki, for their contribution to the establishment of the fundamental concepts of this investigation. We also thank Ms. Tamayo Hatayama, Minako Kato, Naomi Miyahara, Shoko Yamamoto, Keiko Kimura, Tomoko Sueishi and Yoshiko Yamashita for their technical assistance. This study was supported in part by Special Coordination Funds for Promoting Science and Technology (H18-1-3-3-1, Comprehensive approach on asbestos-related diseases), Takeda Science Foundation, grants from the Ministry of Education, Culture, Sports, Science and Technology of Japan (20390178 and 22700933), Ryobi Teien Memory Foundation, The Promotion and Mutual Aid Corporation for Private Schools of Japan, Kawasaki Medical School Project Grants (21-201), Program to disseminate tenure tracking system (FY 2011-2013) from the Ministry of Education, Culture, Sports, Science and Technology of Japan, and Strategic Research Foundation Grant-aided Project for Private Universities from Ministry of Education, Culture, Sport, Science, and Technology, Japan.

References

1. Pan XL, Day HW, Wang W, Beckett LA and Schenker MB: Residential proximity to naturally occurring asbestos and mesothelioma risk in California. Am J Respir Crit Care Med 172: 1019-1025, 2005.
2. Kurumatani N and Kumagai S: Mapping the risk of mesothelioma due to neighborhood asbestos exposure. Am J Respir Crit Care Med 178: 624-629, 2008.
3. Heintz NH, Janssen-Heininger YM and Mossman BT: Asbestos, lung cancers, and mesotheliomas: from molecular approaches to targeting tumor survival pathways. Am J Respir Cell Mol Biol 42: 133-139, 2010.
4. LaDou J, Castleman B, Frank A, *et al*: The case for a global ban on asbestos. Environ Health Perspect 118: 897-901, 2010.
5. Ueki A, Yamaguchi M, Ueki H, *et al*: Polyclonal human T-cell activation by silicate in vitro. Immunology 82: 332-335, 1994.
6. Aikoh T, Tomokuni A, Matsukii T, *et al*: Activation-induced cell death in human peripheral blood lymphocytes after stimulation with silicate *in vitro*. Int J Oncol 12: 1355-1359, 1998.
7. Nishimura Y, Miura Y, Maeda M, *et al*: Impairment in cytotoxicity and expression of NK cell- activating receptors on human NK cells following exposure to asbestos fibers. Int J Immunopathol Pharmacol 22: 579-590, 2009.
8. Nishimura Y, Maeda M, Kumagai N, Hayashi H, Miura Y and Otsuki T: Decrease in phosphorylation of ERK following decreased expression of NK cell-activating receptors in human NK cell line exposed to asbestos. Int J Immunopathol Pharmacol 22: 879-888, 2009.
9. Kumagai-Takei N, Nishimura Y, Maeda M, *et al*: Effect of asbestos exposure on differentiation of cytotoxic T lymphocytes in mixed lymphocyte reaction of human peripheral blood mononuclear cells. Am J Respir Cell Mol Biol 49: 28-36, 2013.
10. Nishimura Y, Maeda M, Kumagai-Takei N, *et al*: Altered functions of alveolar macrophages and NK cells involved in asbestos-related diseases. Environ Health Prev Med 18: 198-204, 2013.
11. Miyoshi I, Kubonishi I, Yoshimoto S, *et al*: Type C virus particles in a cord T-cell line derived by co-cultivating normal human cord leukocytes and human leukaemic T cells. Nature 294: 770-771, 1981.
12. Maeda M, Miura Y, Nishimura Y, *et al*: Immunological changes in mesothelioma patients and their experimental detection. Clin Med Circ Respirat Pulm Med 2: 11-17, 2008.
13. Hyodoh F, Takata-Tomokuni A, Miura Y, *et al*: Inhibitory effects of anti-oxidants on apoptosis of a human polyclonal T-cell line, MT-2, induced by an asbestos, chrysotile-A. Scand J Immunol 61: 442-448, 2005.
14. Miura Y, Nishimura Y, Katsuyama H, *et al*: Involvement of IL-10 and Bcl-2 in resistance against an asbestos-induced apoptosis of T cells. Apoptosis 11: 1825-1835, 2006.
15. Nishimura Y, Miura Y, Maeda M, *et al*: Expression of the T cell receptor Vbeta repertoire in a human T cell resistant to asbestos-induced apoptosis and peripheral blood T cells from patients with silica and asbestos-related diseases. Int J Immunopathol Pharmacol 19: 795-805, 2006.
16. Maeda M, Chen Y, Kumagai-Takei N, *et al*: Alteration of cytoskeletal molecules in a human T cell line caused by continuous exposure to chrysotile asbestos. Immunobiology 218: 1184-1191, 2013.
17. Maeda M, Yamamoto S, Chen Y, *et al*: Resistance to asbestos-induced apoptosis with continuous exposure to crocidolite on a human T cell. Sci Total Environ 429: 174-182, 2012.
18. Maeda M, Nishimura Y, Hayashi H, *et al*: Reduction of CXC chemokine receptor 3 in an in vitro model of continuous exposure to asbestos in a human T-cell line, MT-2. Am J Respir Cell Mol Biol 45: 470-479, 2011.
19. Maeda M, Nishimura Y, Hayashi H, *et al*: Decreased CXCR3 expression in $CD4^+$ T cells exposed to asbestos or derived from asbestos-exposed patients. Am J Respir Cell Mol Biol: 795-803, 2011.
20. Chen S, Ishii N, Ine S, *et al*: Regulatory T cell-like activity of $Foxp3^+$ adult T cell leukemia cells. Int Immunol 18: 269-277, 2006.
21. Sakaguchi S, Miyara M, Costantino CM and Hafler DA: $FOXP3^+$ regulatory T cells in the human immune system. Nat Rev Immunol 10: 490-500, 2010.
22. Flavell RA, Sanjabi S, Wrzesinski SH and Licona-Limon P: The polarization of immune cells in the tumour environment by TGFbeta. Nat Rev Immunol: 554-567, 2010.
23. Kohyama N, Shinohara Y and Suzuki Y: Mineral phases and some reexamined characteristics of the International Union Against Cancer standard asbestos samples. Am J Ind Med 30: 515-528, 1996.
24. Brummelkamp TR, Bernards R and Agami R: A system for stable expression of short interfering RNAs in mammalian cells. Science 296: 550-553, 2002.
25. Bridge AJ, Pebernard S, Ducraux A, Nicoulaz AL and Iggo R: Induction of an interferon response by RNAi vectors in mammalian cells. Nat Genet 34: 263-264, 2003.
26. Naldini L, Blomer U, Gallay P, *et al*: In vivo gene delivery and stable transduction of nondividing cells by a lentiviral vector. Science 272: 263-267, 1996.
27. Zufferey R, Nagy D, Mandel RJ, Naldini L and Trono D: Multiply attenuated lentiviral vector achieves efficient gene delivery in vivo. Nat Biotechnol 15: 871-875, 1997.
28. Arnulf B, Villemain A, Nicot C, *et al*: Human T-cell lymphotropic virus oncoprotein Tax represses TGF-beta 1 signaling in human T cells via c-Jun activation: a potential mechanism of HTLV-I leukemogenesis. Blood 100: 4129-4138, 2002.
29. Li MO, Wan YY, Sanjabi S, Robertson AK and Flavell RA: Transforming growth factor-beta regulation of immune responses. Annu Rev Immunol 24: 99-146, 2006.
30. Zhang W and Liu HT: MAPK signal pathways in the regulation of cell proliferation in mammalian cells. Cell Res 12: 9-18, 2002.
31. Letterio JJ: TGF-beta signaling in T cells: roles in lymphoid and epithelial neoplasia. Oncogene 24: 5701-5712, 2005.

32. Li L, Iwamoto Y, Berezovskaya A and Boussiotis VA: A pathway regulated by cell cycle inhibitor $p27^{Kipl}$ and checkpoint inhibitor Smad3 is involved in the induction of T cell tolerance. Nat Immunol 7: 1157-1165, 2006.
33. Delisle JS, Giroux M, Boucher G, *et al*: The TGF-beta-Smad3 pathway inhibits CD28-dependenT cell growth and proliferation of CD4 T cells. Genes Immun 14: 115-126, 2013.
34. Yoshimura A, Wakabayashi Y and Mori T: Cellular and molecular basis for the regulation of inflammation by TGF-beta. J Biochem 147: 781-792, 2010.
35. Zhu H, Kavsak P, Abdollah S, Wrana JL and Thomsen GH: A SMAD ubiquitin ligase targets the BMP pathway and affects embryonic pattern formation. Nature 400: 687-693, 1999.
36. Wrzesinski SH, Wan YY and Flavell RA: Transforming growth factor-beta and the immune response: implications for anticancer therapy. Clin Cancer Res 13: 5262-5270, 2007.
37. Suzuki E, Kim S, Cheung HK, *et al*: A novel small-molecule inhibitor of transforming growth factor beta type I receptor kinase (SM16) inhibits murine mesothelioma tumor growth in vivo and prevents tumor recurrence after surgical resection. Cancer Res 67: 2351-2359, 2007.
38. Zou W: Regulatory T cells, tumour immunity and immunotherapy. Nat Rev Immunol 6: 295-307, 2006.
39. Fujii M, Toyoda T, Nakanishi H, *et al*: TGF-beta synergizes with defects in the Hippo pathway to stimulate human malignant mesothelioma growth. J Exp Med 209: 479-494, 2012.
40. Murakami S, Nishimura Y, Maeda M, *et al*: Cytokine alteration and speculated immunological pathophysiology in silicosis and asbestos-related diseases. Environ Health Prev Med 14: 216-222, 2009.
41. Derynck R and Zhang YE: Smad-dependent and Smad-independent pathways in TGF-beta family signalling. Nature 425: 577-584, 2003.
42. Brown KA, Pietenpol JA and Moses HL: A tale of two proteins: differential roles and regulation of Smad2 and Smad3 in TGF-beta signaling. J Cell Biochem 101: 9-33, 2007.
43. Siegel PM and Massague J: Cytostatic and apoptotic actions of TGF-beta in homeostasis and cancer. Nat Rev Cancer 3: 807-821, 2003.
44. Levy L and Hill CS: Alterations in components of the TGF-beta superfamily signaling pathways in human cancer. Cytokine Growth Factor Rev 17: 41-58, 2006.
45. Xiao YQ, Freire-de-Lima CG, Schiemann WP, Bratton DL, Vandivier RW and Henson PM: Transcriptional and translational regulation of TGF-beta production in response to apoptotic cells. J Immunol 181: 3575-3585, 2008.
46. Huber S, Schrader J, Fritz G, *et al*: P38 MAP kinase signaling is required for the conversion of $CD4^{+}CD25^{-}$ T cells into iTreg. PLoS One 3: e3302, 2008.
47. Calabro L, Morra A, Fonsatti E, *et al*: Tremelimumab for patients with chemotherapy-resistant advanced malignant mesothelioma: an open-label, single-arm, phase 2 trial. Lancet Oncol 14: 1104-1111, 2013.